Click Here for Full Article

Exploring the sensitivity of interannual basin-scale air-sea CO_2 fluxes to variability in atmospheric dust deposition using ocean carbon cycle models and atmospheric CO_2 inversions

Prabir K. Patra,[1] J. Keith Moore,[2] Natalie Mahowald,[3] Mitsuo Uematsu,[4] Scott C. Doney,[5] and Takakiyo Nakazawa[6]

[1] Estimates of sources/sinks of carbon dioxide (CO_2) at the Earth's surface are commonly made using atmospheric CO_2 inverse modeling, terrestrial and oceanic biogeochemical modeling, and inventory-based studies. In this study, we compare sea-air CO_2 fluxes from the Time-Dependent Inverse (TDI) atmosphere model and the marine Biogeochemical Elemental Cycling (BEC) model to study the processes involved in ocean carbon cycling at subbasin scales. A dust generation and transport model, based on analyzed meteorology and terrestrial vegetation cover, is also used to estimate the interannual variability in dust and iron deposition to different ocean basins. Overall, a fairly good agreement is established between the TDI and BEC model results for the net annual patterns and seasonal cycle of sea-air CO_2 exchange. Sensitivity studies with the ocean biogeochemical model using increased or reduced atmospheric iron inputs indicate the relative sensitivity of air-sea CO_2 exchange. The simulated responses to changes in iron inputs are not instantaneous (peak response after $\sim 2-3$ years). The TDI model derived seasonal cycles for the Southern Ocean (South Atlantic) are better matched by the BEC model by increasing (decreasing) iron inputs through atmospheric aerosols. Our results suggest that some of the interannual variability in TDI model air-sea CO_2 fluxes during the past decade may be explainable by dust variability that relaxes/increases iron limitation in high-nitrate, low-chlorophyll (HNLC) ocean regions.

1. Introduction

[2] Understanding the evolution of the global carbon cycle is challenging because the future atmospheric CO_2 burden is governed by the interplay of fossil fuel emissions, land-use change, land and ocean CO_2 sinks, and climate [*Prentice et al.*, 2001]. Several studies have suggested that poorly constrained, climate-carbon cycle feedbacks may amplify anthropogenic climate change on multidecadal to centennial timescales [e.g., *Cox et al.*, 2000; *Fung et al.*, 2005; *Friedlingstein et al.*, 2006]. This is important since

the policies to mitigate atmospheric CO_2 rise and slow global warming could suffer setbacks if proper measures of the biospheric release and uptake of carbon due to the climate variability and climate change are not taken into account [*Dilling et al.*, 2003]. Historical observational data, such as atmospheric CO_2, meteorological and biospheric parameters, can be used to quantify climate-carbon cycle interactions on interannual to decadal timescales. Significant progress has been made in understanding the global and regional CO_2 flux variations due to the climate variations leading to physical, chemical and biological changes in the ocean and land biospheres [e.g., *Keeling et al.*, 1995; *Bousquet et al.*, 2000; *Lucht et al.*, 2002; *Roedenbeck et al.*, 2003; *Nemani et al.*, 2003; *McKinley et al.*, 2004; *Peylin et al.*, 2005; *Patra et al.*, 2005a, 2005b]. For land regions, an overall agreement is found regarding the reduction in uptake or a net source of carbon during periods with drier, warmer, and more frequent fire conditions, though disagreements exist in flux amplitudes [see *Bousquet et al.*, 2000; *Le Quéré et al.*, 2003; *Roedenbeck et al.*, 2003; *Patra et al.*, 2005b; *Ciais et al.*, 2005; *van der Werf et al.*, 2006]. However, much less is understood about the causes for oceanic CO_2 flux variabilities during the 1990s at the global scale (see *Le Quéré et al.* [2003] and *Patra et al.* [2005a] for

[1] Frontier Research Center for Global Change, JAMSTEC, Yokohama, Japan.
[2] Earth System Science, University of California, Irvine, California, USA.
[3] National Center for Atmospheric Research, Boulder, Colorado, USA.
[4] Center for International Cooperation, Ocean Research Institute, University of Tokyo, Tokyo, Japan.
[5] Department of Marine Chemistry and Geochemistry, Woods Hole Oceanographic Institution, Woods Hole, Massachusetts, USA.
[6] Center for Atmospheric and Oceanic Studies, Tohoku University, Sendai, Japan.

discussion). At the regional scale, strong flux variability in the Tropical Pacific is related to ENSO [e.g., *Feely et al.*, 1999; *Takahashi et al.*, 2003; *Obata and Kitamura*, 2003; *Wetzel et al.*, 2005], and a number of studies have explored the ocean response to extratropical regional climate modes (i.e., North Atlantic Oscillation, Pacific Decadal Oscillation, Antarctic Circumpolar Wave) [e.g., *Gruber et al.*, 2002; *Dore et al.*, 2003; *Le Quéré et al.*, 2000; *McKinley et al.*, 2004; *Patra et al.*, 2005a; *McKinley et al.*, 2006].

[3] An interesting component of the global carbon cycle is the interactions between land and ocean. There is growing awareness that particulate matter (as mineral dust or bio-mass burning and combustion byproducts) emitted from the land regions and deposited over the ocean through the atmospheric transport brings macronutrients and micronu-trients that could change the behavior of oceanic biogeo-chemistry [e.g., *Abram et al.*, 2003; *Jickells et al.*, 2005]. In particular, the atmospheric source of dissolved iron from mineral dust deposition is a key nutrient source for the oceans [*Martin et al.*, 1991; *Fung et al.*, 2000; *Mahowald et al.*, 2005]. Carbon cycle responses to dust deposition have been studied with oceanic biogeochemistry models [e.g., *Moore et al.*, 2004, 2006]. *Moore et al.* [2006] forced a global ocean ecological-biogeochemical model with dust inputs from different climate states and found a strong impact on global-scale export production and air-sea CO$_2$ exchange. Dust inputs also had a strong impact on nitrogen fixation rates, as diazotrophs were limited by iron over much of the low to mid latitude oceans. Thus variations in dust inputs had a strong impact in traditional high-nitrate, low-chlorophyll (HNLC) regions (subpolar North Pacific, equatorial Pacific, Southern Ocean) where the entire phy-toplankton community is iron-limited and in tropical and subtropical areas by modifying rates of nitrogen fixation. This indirect dust-nitrogen fixation-export production link-age had a comparable effect on air-sea CO$_2$ exchange over decadal timescales as the response seen in the HNLC zones [*Moore et al.*, 2006].

[4] Recent studies using satellite ocean color remote sensing illustrate the presence of long-term trends in surface chlorophyll concentrations, particularly in some shelf/coastal areas [e.g., *Gregg et al.*, 2005]. They attributed chlorophyll increases in some regions to a decrease in sea-surface temperature (SST), i.e., increased upwelling, but the overall causes for these increases are largely unknown. For exam-ple, it has been established that the atmospheric aerosols exert cooling near the earth's surface [*Satheesh and Ramanathan*, 2000], which might also lower SST. There is considerable complexity in the land-ocean coupled car-bon cycle system, and anthropogenic influence is perturbing these couplings in numerous ways such as modifications to the hydrologic cycle, deforestation, changing riverine nutri-ent transport to the oceans [e.g., *Asner et al.*, 2005; *Syvitski et al.*, 2005]. Impacts of changes in precipitation and surface temperature on the carbon cycle are already a measurable quantity in the well-observed parts of the world [*Ciais et al.*, 2005; *Angert et al.*, 2005]. The large CO$_2$ net source anomalies, for example, ∼0.5 Pg-C for the Western Europe in 2003, can be corroborated by atmospheric-CO$_2$ inversion results (P. K. Patra, unpublished data, updated inversion, 2005).

[5] In this study we compared atmospheric-CO$_2$ inverse model fluxes (Time-Dependent Inversion; TDI), oceanic model air-sea CO$_2$ fluxes (Biogeochemical Elemental Cycling; BEC), and simulated dust sources, atmospheric transport and deposition (Model of Atmospheric Transport and Chemistry (MATCH)/National Center for Environmental Prediction (NCEP)/Dust Entrainment And Deposition (DEAD)). An attempt is made to explain the similarities and differences between the ocean and atmosphere CO$_2$ results by analyzing the ocean model's sensitivity to iron (Fe) inputs from atmospheric dust deposition. We utilize a combination of an ocean model control, forced with repeat annual cycle of atmospheric physical forcing and dust deposition, and sensitivity studies to a tenfold step function increase or decrease in dust deposition. The TDI, BEC, and DEAD modeling setups are designed for understanding the interannual variations in CO$_2$ fluxes in the context that dust variations significantly impact the marine carbon cycle.

2. Materials and Methods

2.1. Time-Dependent Inversion (TDI) of Atmospheric CO$_2$

[6] We have used a time-evolving, atmospheric transport inverse model (TDI) for estimating surface CO$_2$ sources and sinks (i.e., fluxes) [*Rayner et al.*, 1999; *Gurney et al.*, 2004; *Patra et al.*, 2005a, 2005b]. Atmospheric-CO$_2$ data at 87 stations are used for constraining the TDI model simulations, following a preprocessing of actual concentrations reported by several organizations worldwide [*GLOBALVIEW-CO$_2$*, 2004]. The NIES/FRCGC transport model, driven by interannually varying NCEP/NCAR reanalyzed meteorology, is used for forward simulations (see *Patra et al.* [2005a] for detailed description). The estimated inverse model fluxes generally respond to climate oscillations at global and region scales, and the global land and ocean CO$_2$ flux anomalies are typically anticorrelated [e.g., *Patra et al.*, 2005a, 2005b]. In previous inverse studies, the largest ocean flux variability is found in the tropical and northern latitudes [*Rayner et al.*, 1999; *Bousquet et al.*, 2000; *Roedenbeck et al.*, 2003]. However, *Patra et al.* [2005a] found large interannual flux variations for the ocean regions in southern latitudes also. The latter study used a larger measurement network, which helped them to constrain the ocean region fluxes fairly satisfactorily (within respective uncertainty estimates) if compared with the independent oceanic-pCO$_2$ based flux estimates [*Patra et al.*, 2006]. However, no overall agreement could be established with regional flux variability simulated by oceanic biogeochemical models. Typically, the ocean carbon cycle models exhibit much lower extratropical interannual flux variability compared to those estimated using atmospheric data [*Lee et al.*, 1998; *Le Quéré et al.*, 2003; *Patra et al.*, 2005a; *McKinley et al.*, 2006].

[7] Figure 1 shows the TDI average sea-air CO$_2$ fluxes (gC m^{-2} d^{-1}) for the period 1990−2001 and the interan-nual variability in monthly mean fluxes (1σ). To calculate σ-values, we use monthly anomalies from an average sea-sonal cycle for each region. The 1σ values using annual mean fluxes are smaller than those shown here, while the values are significantly greater for the straight monthly variability including the seasonal cycle. Our results indicate that the northern North Pacific, most parts of equatorial Pacific, and southern areas of Pacific and Atlantic all exhibit significant
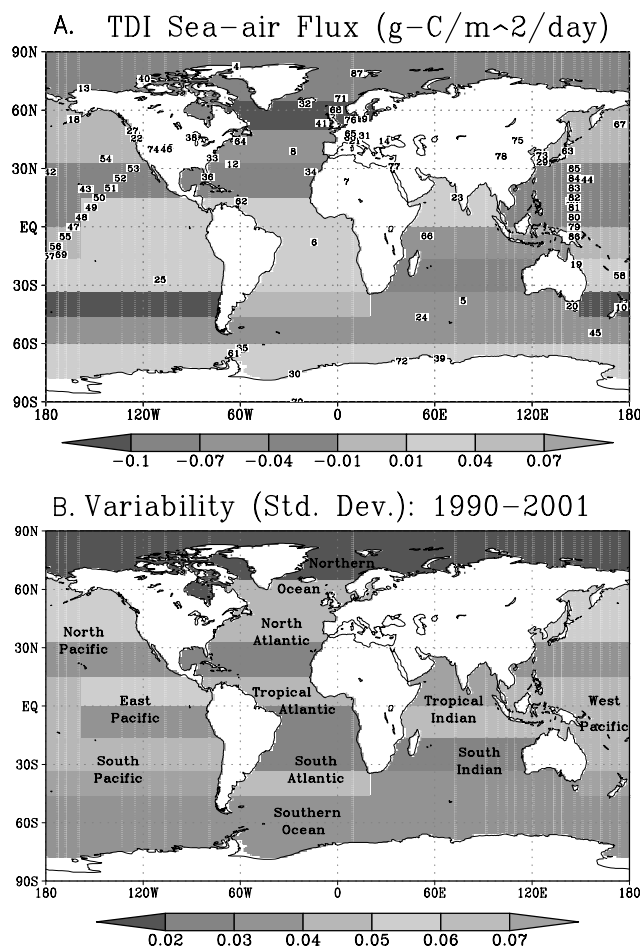
A. TDI Sea-air Flux (g-C/m^2/day)

B. Variability (Std. Dev.): 1990−2001

Figure 1. (a) Average sea-air CO$_2$ fluxes and (b) associated interannual variability estimated using the TDI monthly fluxes for the period 1990−2001. The variability is computed for monthly anomalies after removal of a mean seasonal cycle for each region. The locations of atmospheric CO$_2$ measurement stations as used in this TDI simulation are marked in Figure 1a, and the oceanic region name/division used in discussion below are given in Figure 1b. The average CO$_2$ fluxes are the same as those of *Patra et al.* [2005a], but are depicted in different units (per unit area rather than per inverse model region), for comparison with ocean model simulations.

variability in CO$_2$ fluxes per unit area. Because of its large area, the northern portion of the Southern Ocean also shows large CO$_2$ flux variability if the fluxes are integrated to whole regions (i.e., Pg C yr^{-1}). The greater flux variability in the Tropical Indian Ocean is an artifact of atmospheric-CO$_2$ data error at the Seychelles station prior to 1996.

2.2. Dust Transport and Deposition Model

[8] Mineral aerosols were simulated using a three-dimensional chemical transport model based on National Centers for Environmental Prediction/National Center for Atmospheric Research (NCEP/NCAR) reanalysis for the years 1988−2004 [*Kistler et al.*, 2001]. The dust source and deposition scheme is based on the Dust Entrainment and Deposition (DEAD) scheme [*Zender et al.*, 2003], and the chemical transport model was the Model of Atmospheric Transport and Chemistry (MATCH) [*Rasch et al.*, 1997],

which has been developed specifically to be used with reanalysis winds [*Mahowald et al.*, 1997]. The dust source areas are defined as dry, poorly vegetated regions which have easily erodible sources, using topographic lows as preferential sources areas [*Ginoux et al.*, 2001]. Dust is removed by wet deposition during precipitation events, and by dry deposition from gravitational settling and turbulent processes. The model is described in more detail elsewhere [*Zender et al.*, 2003; *Luo et al.*, 2003; *Mahowald et al.*, 2002, 2003]

[9] The mean climatology of the dust model was compared to available observations (e.g., in situ concentration, in situ optical depth, deposition data and satellite optical depth) in detail by *Luo et al.* [2003], which showed that the model is able to capture the mean seasonal cycle and distribution of the aerosols fairly well, although with somewhat reduced skill in the Southern Hemisphere. The ability of the model to capture daily and interannual variability was also examined in detail in previous studies [e.g., *Mahowald et al.*, 2002, 2003; *Hand et al.*, 2004]. Generally speaking the model can obtain statistically significant in correlations between monthly averages at the few available (∼10) in situ dust concentration stations [*Mahowald et al.*, 2003, Table 1], although the model has difficulty at some Southern Hemisphere stations (Funafuti and Norfolk Island). Comparison with satellite data is possible; however, this data is more difficult to interpret because mineral aerosols only dominate the aerosol optical depth over some ocean regions [e.g., *Tegen et al.*, 1997]. In these regions, the model appears to be able to capture much, but not all, of the interannual variability [*Mahowald et al.*, 2003, Figure 2].

[10] In addition, the MATCH/NCEP/DEAD simulations appear to have roughly the right amount of interannual variability [*Mahowald et al.*, 2003, Table 2 and Figure 3]. Model analyses have suggested that most of the interannual variability in concentrations downwind of the source regions is driven by transport, (or transport/source correlations) and not by source interannual variability alone [*Tegen and Miller*, 1998; *Mahowald et al.*, 2003]. Model and observational studies over the time period 1979 to 2000 have not shown evidence for global or regional trends in dust source or deposition [e.g., *Mahowald et al.*, 2003] (see review by *Mahowald et al.* [2005]). For this study we are interested in the regional patterns of interannual variability in deposition. However, there are very few sites where deposition per se is measured (and not inferred from surface concentrations, which ignores the important wet deposition component), and there are no deposition data sets with multiple years. Model results represent, perhaps, our best state of understanding for interannual variability in dust deposition to ocean regions, but they cannot be considered definitive. Figure 2 shows the average dust deposition and fractional interannual variability (given as a coefficient of variation: standard deviation divided by the mean) in the period 1990−2001. Note that the fractional variability is largest over the ocean regions in southern hemisphere mid−high latitudes and the North Atlantic.

2.3. Biogeochemical Modeling of Air-Sea CO$_2$ Fluxes

[11] One possible mechanism of larger input of micronutrients such as iron to the HNLC regions (see Figure 3) is the enhanced transport of soil and mineral dusts from the
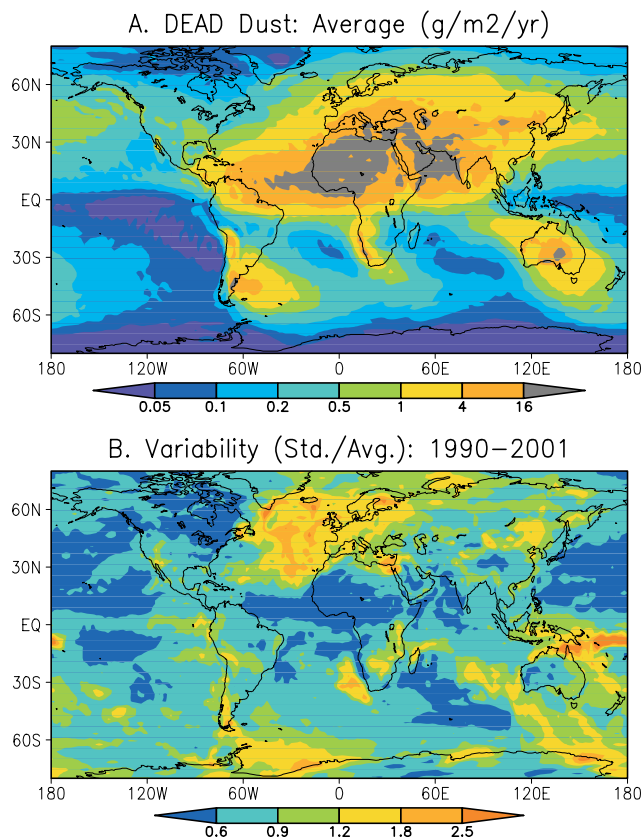
Figure 2. Spatial maps of average dust deposition and fractional variability (standard deviation divided by mean) in dust deposition (period: 1990–2001) from the MATCH/NCEP/DEAD model simulations. The variability is shown as the average of 1σ values in monthly deposition over 12 years.

land to the ocean through the atmosphere. To test the effect of dust input variations on sea-air CO_2 fluxes and associated biogeochemical processes, we used a coupled ocean Biogeochemical Elemental Cycling (BEC) model developed at NCAR, UC Irvine and WHOI [*Moore et al.*, 2004]. The model runs within the NCAR Community Climate System Model (CCSM3) [*Collins et al.*, 2006] utilizing the Parallel Ocean Program (POP) ocean circulation component [see *Moore et al.*, 2004, 2006, and references therein]. The salient features of the model are multiple potentially growth-limiting nutrients and explicit iron cycling in the oceans with external sources from mineral dust and continental shelves and four functional groups of phytoplankton: diatoms, diazotrophs, coccolithophores, and picoplankton. Thus, as dust deposition varies, the model captures the shifts in community composition and biogeochemical rates observed in deliberate iron-fertilization experiments in HNLC regions and in low-latitude regimes with significant nitrogen fixation [*Moore et al.*, 2006]. The BEC model includes external iron sources from mineral dust deposition and a crude sedimentary source in shallow ocean regions (constant diffusive flux where ocean depth <1100 m [*Moore et al.*, 2004]). While it is believed that dust inputs are the dominant source to the open ocean, the continental iron signal can at times influence areas far from shore [*Johnson et al.*, 1997; *Lam et al.*, 2006]. Variability in this

offshore transport of sedimentary-derived iron is not accounted for in the present study.

[12] The sensitivity of ocean biogeochemistry and air-sea CO_2 exchange to changes in mineral dust deposition to the oceans is studied with three model simulations: Case-x1 using climatological dust deposition from the MATCH/NCEP/DEAD simulations (see Figure 2a); Case-x10 using ten times the rate of climatological dust deposition; and Case-x0.1 using one tenth of climatological dust deposition. Dust deposition used here is the monthly mean values from *Luo et al.* [2003]. For our case studies the BEC model was integrated first for 1000 years with climatological dust forcing and atmospheric CO_2 fixed at a pre-industrial value of 278 ppm. The model was then integrated for an additional 24 years with atmospheric CO_2 increased to 350 ppm, to partially allow the model to equilibrate to 1990s conditions. Three branch simulations were conducted from the end of the spin-up solution for an additional 24 years with seasonally varying climatological dust (Case-x1) and climatology dust modified by factors of 0.1 (Case-x0.1) and 10.0 (Case-x10) (see Figure 3 for a schematic diagram). These simulations were designed to set reasonable upper and lower bounds on the variations in atmospheric dust inputs to the oceans during the period of our atmospheric inversion (1997–2001) given the large uncertainties in both deposition rates and iron solubility. Here we assume for all simulations a constant 3.5% of dust is iron and that 2% of this is soluble. We seek to test whether interannual variations in dust deposition within these bounds could significantly impact air-sea CO_2 exchange. On longer decadal to centennial timescales, ocean CO_2 storage will be affected by dust-driven reorganizations in subsurface nutrient and dissolved inorganic carbon fields [*Boyd and Doney*, 2002].

3. Results

3.1. BEC Model Simulation Results

[13] Figure 4 shows the temporal evolution of CO_2 fluxes and associated biogeochemical fluxes from the beginning of the branching simulations with atmospheric CO_2 concentration prescribed at 350 ppm. The rate of total CO_2 draw down by the ocean from the atmosphere is significantly increased with the increase in dust deposition. This draw down is triggered by the enhanced primary and export production (increased sinking Particulate Organic Carbon, POC). Though the maximum change in global air-sea CO_2 flux is observed in the first few years of the model simulations, there is still an offset at the end of the runs. At year 24 the oceanic sink due to 10 times enhanced dust input (Case-x10) is about 0.9 Pg-C yr^{-1} greater compared to that corresponding to climatological dust input (Case-x1), and the one-tenth dust input run (Case-x0.1) results in an effective net outgassing of CO_2 with a similar offset compared to Case-x1. This indicates that an increase (decrease) in iron inputs to the ocean can act to drive significant enhanced (reduced) uptake of atmospheric CO_2 by the oceans at interdecadal timescales, with the strongest impact in the first few years as found previously [*Moore et al.*, 2006]. Corresponding to the increase (decrease) in iron inputs, the nitrogen fixation and denitrification rates have also increased (decreased) dramatically. Such changes are
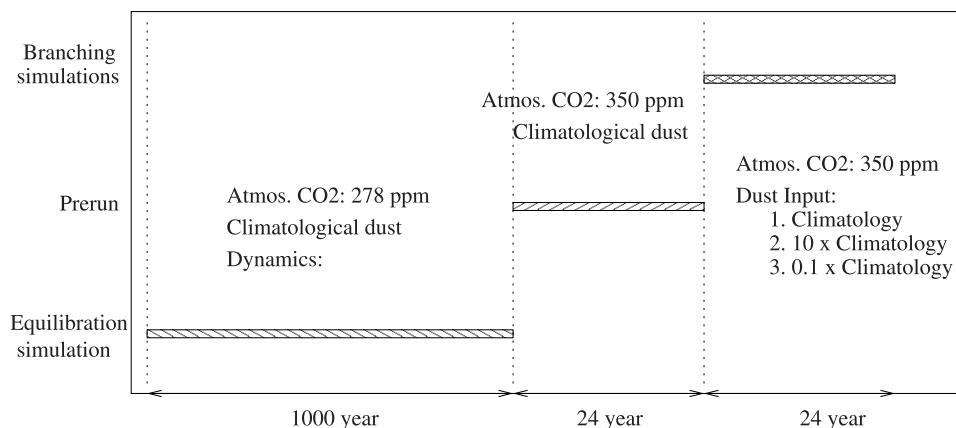
Figure 3. Schematic depicting the time period and types of BEC model simulations (see text for details).

also likely to have influence on other greenhouse gases such as nitrous oxide (N_2O), methane (CH_4) and the other chemical constituents with climate impact, for example, dimethyl sulphide (DMS). However, these gases are not currently simulated by the BEC model, and a detailed discussion on this issue is beyond the scope of this study. As our main focus is on interannual timescales, the BEC model results from year 1 following the step-function dust perturbations are used to explore the impact of dust on interannual CO_2 flux variations as derived by the time-dependent inverse (TDI) model of atmospheric CO_2. The results 5 years following the dust perturbations are mainly used for explaining the spatial patterns and magnitudes in the annual net TDI model derived CO_2 fluxes for different regions. For comparison, the changes in oceanic uptake at 1 or 5 year of the BEC model simulations due the changes in dust flux are larger than the TDI model estimated increase in oceanic CO_2 flux (∼1.0 Pg-C) during the 1990s [*Patra et al.*, 2005a]. The drastic changes in dust deposition in our perturbation experiments would have strong "downstream" impacts on biogeochemistry over decadal and longer timescales as subsurface nutrient pools were altered owing to changes in the strength of the biological pump [i.e., *Boyd and Doney*, 2002; *Sarmiento et al.*, 2004].

[14] The variations in atmospheric iron inputs in the three simulations have a profound influence on ocean biogeo-
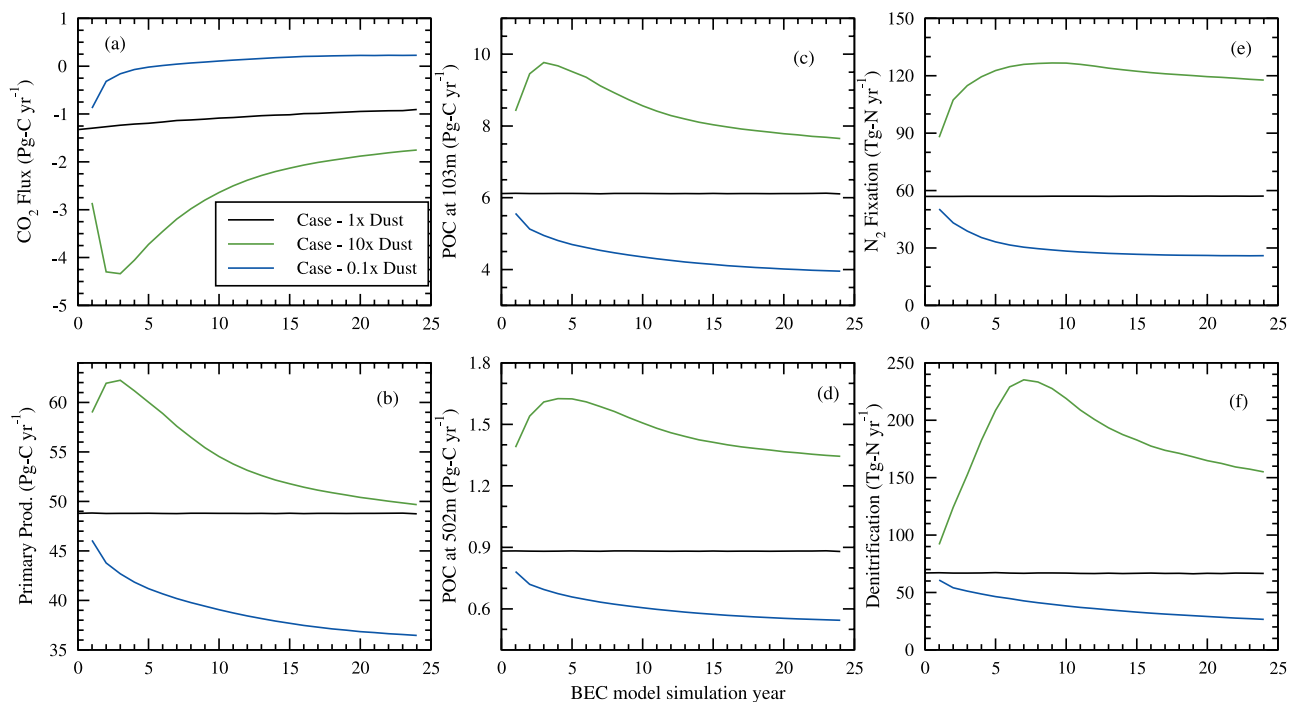

Figure 4. Time evolution of (a) sea-air CO_2 flux, (b) surface layer primary productivity, sinking particulate organic carbon (POC) at (c) 103 m depth and (d) 502 m depth, (e) nitrogen fixation, and (f) denitrification rate during the 24 years of the branching simulations with the three different cases of dust input.
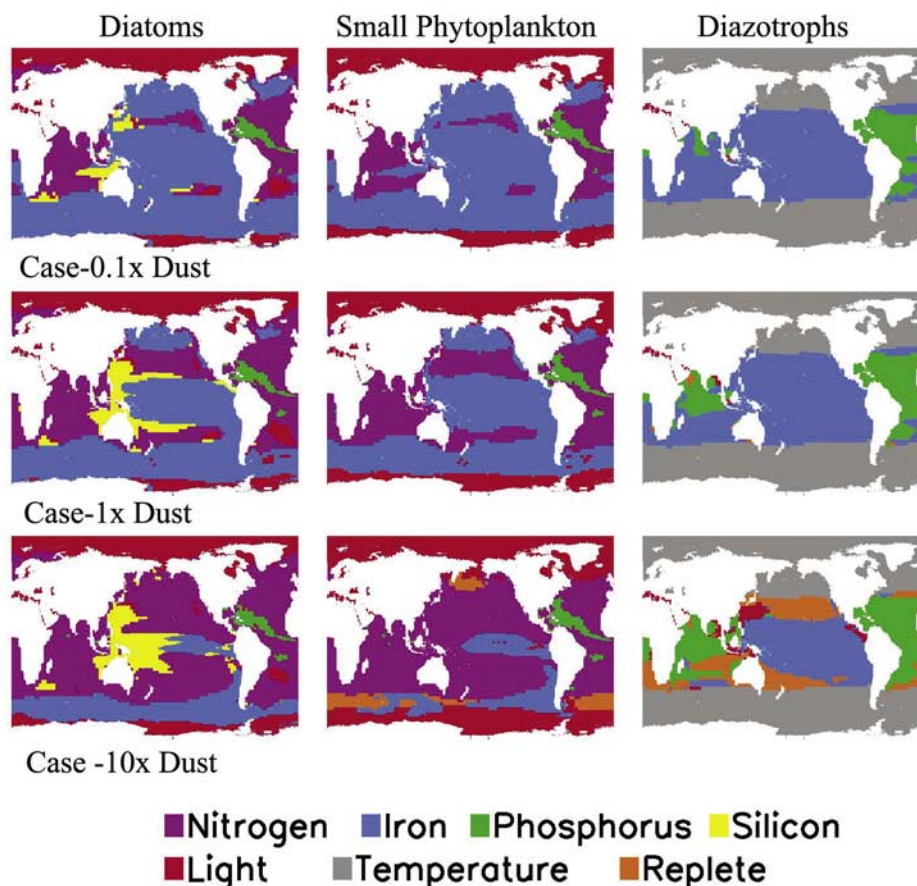
Figure 5. Latitude-longitude distributions of the factor most limiting annual phytoplankton growth rates for small phytoplankton, diatoms, and diazotrophs at year 5 of the BEC dust-sensitivity branching simulations.

chemical fluxes (Figure 4) and on the patterns of nutrient limitation for the different phytoplankton functional groups. The most limiting factor for growth at the annual timescale is plotted for year 5 of our simulations for the diatom, small phytoplankton, and diazotroph phytoplankton groups in Figure 5. The iron-limited areas for the diatoms and small phytoplankton change dramatically between the three simulations, reflecting the large perturbations in the Case-x0.1 and Case-x10 simulations. The diazotrophs are mainly iron-limited at the low to mid latitudes, although the areas where growth is phosphorus limited expand with increasing iron inputs (Figure 5). Note that in many areas where the diazotrophs are iron-limited the other phytoplankton groups are nitrogen limited. This gives these regions a sensitivity to atmospheric iron inputs normally associated only with the HNLC regions [*Moore et al.*, 2006]. These results highlight the dynamic nature of oceanic nutrient limitation regimes and the strong sensitivity to variations in mineral dust deposition.

3.2. Spatial Distributions of Dust Input and CO$_2$ Fluxes

[15] Figure 6 shows a comparison of spatial distributions of CO$_2$ fluxes using the three dust input strengths (Figures 6b, 6c, and 6d) with the estimates of ship-borne estimates of CO$_2$ fluxes (Figure 6a) [*Takahashi et al.*, 2002] (values updated in 2003; referred to as TT03). The TDI estimated sea-air flux distribution can be seen in Figure 1a. The CO$_2$ flux distributions from ocean BEC control simulations are broadly consistent with ocean observations and atmospheric inverse estimates. The major differences are observed in the Southern Ocean region, where the BEC model produces less uptake of carbon by the ocean compared to those estimated using the TDI model and ship-borne measurements; in part this reflects the fact that the ocean simulations are conducted with a constant, rather than transient, increasing atmospheric CO$_2$ concentration. Examining the different BEC simulations, the strong impact of iron inputs in the HNLC regions is apparent. Strong decreases in the flux of CO$_2$ to the atmosphere are seen in the Case-x10 simulation relative to the climatological dust run in the Southern Ocean, the equatorial Pacific, and the subarctic Pacific. Similarly, increased sea-air flux is seen in these same regions under the low Case-x0.1 dust flux.

[16] The net air-sea fluxes (uptake) for the global ocean are 1.46 Pg-C yr^{-1} from TT03 corresponding to a climatological year 1995 and 1.87 ± 0.52 Pg-C yr^{-1} from the TDI model for the period 1988–2001. The BEC modeled air-sea fluxes 1 year following the step-function dust perturbations are 1.14, 0.73 and 2.72 Pg-C yr^{-1} corresponding to clima-
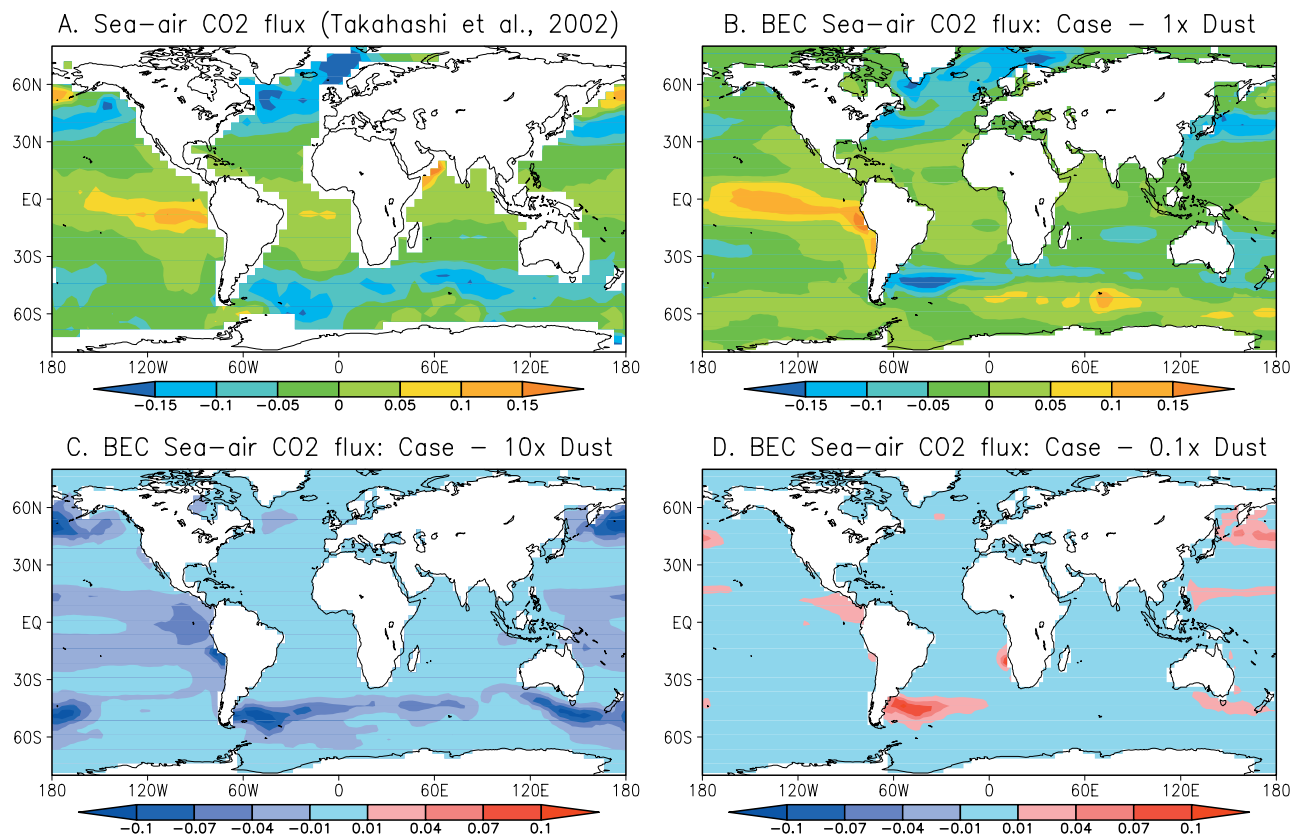
Figure 6. Distributions of annual mean sea-air fluxes of CO_2 (in g-C m^{-2} d^{-1}) simulated using the BEC model with varying dust Fe input; (b) climatological dust (Case-1x), and relative changes in CO_2 fluxes (c) at 10 times dust input (Case-10x) and (d) at one-tenth dust input (Case-0.1x). (a) An updated flux distribution of *Takahashi et al.* [2002] data, for a comparison of spatial pattern in sea-air exchanges.

tological dust input, one-tenth and ten times climatological dust cases, respectively. The global net ocean carbon uptakes 5 years following the dust perturbations are 1.04, 0.11, and 3.68 Pg-C yr^{-1}, respectively. Since we have not run an ocean simulation with transient increasing atmospheric CO_2, we cannot directly compare absolute uptake to the atmospheric inversion and in situ observational data, but we can compare the large changes in CO_2 uptake across the dust sensitivity experiments relative to the control case. The carbon uptake response to the step-function dust input perturbations maximize at about 4–5 years, with a tendency to level out at a new quasi-equilibrium level by the end of the simulations (year 24). The new state of quasi-equilibrium, however, depends on the dust input level; decreased (increased) carbon uptake is found for reduced (elevated) dust input.

3.3. Comparison of Regional TDI and BEC Model Fluxes

[17] Table 1 shows the comparison of sea-air fluxes of CO_2 at regional (subbasin) scale between different estimation scenarios depicted in Figure 6. Though the BEC model simulated fluxes are within the uncertainty range of TDI estimated fluxes, the average values differ significantly. HNLC regions are typically linked to low Fe inputs, particularly in the tropical Pacific and the Southern Ocean [*Fung et al.*, 2000]. The largest CO_2 exchange responses to changes in dust input are also linked to low Fe input regions

[*Moore et al.*, 2006]. By increasing the Fe input to 26 Gg yr^{-1} (from 2.6 Gg yr^{-1}), the East Pacific source is reduced to 0.38 and 0.06 Pg-C yr^{-1} (from about 0.71 Pg-C yr^{-1}) at the end of 1 and 5 years of BEC model Case-x10 dust simulation, respectively. The year 1 response reflects the increased iron input from the atmosphere, while the year 5 response reflects also a drift in subsurface iron concentrations. Similarly, large increases in CO_2 uptake in the Southern Ocean region are simulated with the increases in Fe. However, the response of Southern Ocean uptake to the Fe increase is fairly slow; for example the net increase in uptake in Case-x10 at the end of 1 year is about 0.3 Pg-C yr^{-1} and at 5 years is about 1.1 Pg-C yr^{-1}. This suggests that the full biogeochemical cycling of Fe in the Southern Ocean is slower compared to the East Pacific. The direct biological responses to iron fertilization in the model happen on timescales of about a season. The longer timescales reflect changes in ocean iron reservoirs. The primary supply of Fe to the surface in the Southern Ocean comes from upwelling of subsurface Fe [*Archer and Johnson*, 2000; *Fung et al.*, 2000], and the slow biogeochemical response to atmospheric dust deposition reflects the more gradual buildup of subsurface iron in this region of deep mixing. The range of CO_2 fluxes obtained for the three different BEC model scenarios 1 and 5 years following the dust input perturbations fully encompass the averages of regional CO_2 fluxes estimated by the TDI model or TT03.

[18] Considerable uncertainty surrounds the magnitude of atmospheric dust inputs to the ocean and the subsequent

Table 1. Comparison of Regional-Scale Integrated Fluxes as Derived by *Takahashi et al.* [2002], *Patra et al.* [2006], and Ocean BEC Model Simulations for the Three Dust Input Cases 1 and 5 Years After the Step-Function Perturbation[a]

Region Name	TT03 Flux	TDI Flux	TDI Uncertainty	BEC Dust Cases: Year 1 Climatology	One Tenth	Ten Times	BEC Dust Cases: Year 5 Climatology	One Tenth	Ten Times	Climatological Fe Input
North Pacific	−0.48	−0.28	0.56	−0.60	−0.50	−0.87	−0.59	−0.37	−0.65	0.39
West Pacific	0.10	−0.08	0.45	0.05	0.09	−0.14	0.05	0.19	−0.16	0.13
East Pacific	0.59	0.36	0.54	0.70	0.76	0.38	0.72	0.87	0.06	0.09
South Pacific	−0.26	−0.55	0.71	−0.33	−0.29	−0.54	−0.32	−0.13	−0.56	0.21
Northern Ocean	−0.30	−0.37	0.30	−0.36	−0.36	−0.38	−0.36	−0.34	−0.36	0.16
North Atlantic	−0.28	−0.30	0.44	−0.21	−0.21	−0.22	−0.20	−0.20	−0.21	2.03
Trop. Atlantic	0.17	0.15	0.49	0.07	0.08	0.07	0.08	0.10	0.08	4.79
South Atlantic	−0.13	0.06	0.58	−0.28	−0.18	−0.37	−0.27	−0.03	−0.34	0.66
Southern Ocean	−0.55	−0.38	0.79	0.24	0.27	−0.06	0.25	0.31	−0.85	0.16
Tropical Indian	0.17	−0.05	0.77	−0.09	−0.08	−0.10	−0.08	−0.04	−0.09	2.79
South Indian	−0.47	−0.43	0.55	−0.32	−0.30	−0.45	−0.31	−0.24	−0.57	0.32

[a]*Takahashi et al.* [2002] is denoted by TT03: 2003 updated values and corresponds to 1995; *Patra et al.* [2006] is denoted by TDI: averaging period is 1988−2001. TT03 fluxes are estimated using gas transfer formulation by *Wanninkhof* [1992] as are the BEC model fluxes. All the values are in Pg-C yr^{-1} except those for climatological Fe input (right column) from atmospheric dust deposition (in mg-Fe m^{-2} yr^{-1}). The "one tenth" or "ten times" Fe input cases can be produced by division or multiplication by 10, respectively.

solubility and bioavailability of iron from dust. Greater iron inputs from the atmosphere than in our dust climatology case would improve the BEC model sea-air CO$_2$ fluxes relative to the TDI in the Southern Ocean, the East and West Pacific, and in the South Pacific. Similarly, reducing iron inputs from our standard run would improve the mismatch in the South Atlantic and the Tropical Indian Ocean. The coastal upwelling zone in the Arabian Sea [*Takahashi et al.*, 2002] is not well captured in the coarse resolution BEC model; the BEC model, in contrast, produces a small uptake in the TIO region. In addition, the TIO region's productivity is not limited by iron, but the macronutrients like phosphate (PO$_4$), silicate (SiO$_4$) or nitrate [*Moore et al.*, 2002, 2004]. Sensitivity to the atmospheric macronutrient inputs to the surface ocean is not included in this work [e.g., *Rengarajan and Sarin*, 2004] but will be the focus of future studies.

3.4. Seasonal Cycle in CO$_2$ Fluxes and Implications for Interannual Variability

[19] On the basis of the atmospheric CO$_2$ observations at 87 stations and a tracer transport model, the seasonal cycles and interannual variations in CO$_2$ fluxes have been derived using the TDI model for 22 partitioned areas of the global ocean [*Patra et al.*, 2005a]. Figure 7 displays the TDI model results (aggregated to 11 regions) and the BEC model simulated seasonal cycles for year 1 of the dust scenarios. Since no interannual variations in physical forcing or dust input are implemented in the BEC model simulations, the BEC seasonal flux cycles repeat each year (referred to as "cyclostationary"). However, the TDI model derived fluxes include the effect of interannual changes in dust on the biogeochemistry and variability in air-sea CO$_2$ flux driven by physics/climate. The seasonal amplitude and phase of the TDI and BEC sea-air CO$_2$ fluxes are in fairly good agreement (within the TDI flux uncertainty estimates on an average) for the North Atlantic, South Indian, North and South Pacific, though the BEC amplitudes tend to be somewhat lower than those from the TDI. For the tropical oceans, both TDI and BEC model simulations suggest only a weak seasonal cycle, if any.

[20] In some regions, the amplitude of the ocean CO$_2$ seasonal cycle and annual mean fluxes are sensitive to dust input. A prominent region of dust sensitivity is the East Pacific (Figure 7c), where the BEC model sensitivity runs

suggest that a greater iron input tends to produce larger seasonal cycles and net CO$_2$ drawdown. The TDI simulations exhibit considerable interannual variability for the East Pacific region but no consistent seasonal cycle. Even factor of 10 changes in atmospheric dust deposition to the BEC simulations, however, would not capture the TDI-derived interannual variability in the East Pacific, which is thought to reflect changes in upwelling associated with ENSO. However, recent model results for aerosol source sectors suggest that biomass burning aerosols could be a source of biology-limiting nutrients to this oceanic region [*Koch et al.*, 2007].

[21] In contrast, elevated iron inputs to the Southern Ocean would both make the BEC model seasonal cycle more similar to the larger amplitudes exhibited by the TDI solutions and help explain the atmospheric derived interannual flux variability estimates. It should be noted here that the Case-10x BEC seasonal cycle amplitude increases significantly from 1.5 Pg-C yr^{-1} (Figure 7k) one year after the dust perturbation to 5.6 Pg-C yr^{-1} (peak at +1.4 Pg-C yr^{-1} and trough at −4.2 Pg-C yr^{-1}) after 5 years of elevated dust (see auxiliary material Figure S1[1]). This indicates that a substantially smaller dust perturbation than a factor of 10 increase could produce the TDI model derived Southern Ocean seasonal cycle and interannual variability. For comparison, the DEAD model exhibits interannual variability in the seasonal maximum dust deposition to the Southern Ocean of roughly a factor of 2 to 5, easily large enough to result in substantial ocean biogeochemical variability.

[22] For the West Pacific, ocean iron is typically not the most limiting factor (nitrogen is), but dust deposition may influence nitrogen fixation rates. The Case-x10 simulation tends to introduce a weak seasonal peak in winter-spring time in agreement with the TDI model. Major dust efflux events to this ocean region from southeast and east Asia are observed during the TDI analysis period [*Uematsu et al.*, 2002]. Much less can be discussed about the TIO seasonal cycle since the signal is a complex mixture of two distinct ocean basins (the Arabian Sea and Bay of Bengal) with different biogeochemical behavior [*Sabine et al.*, 2000]. The South Pacific Ocean seasonal cycles are also not sensitive to

---

[1]Auxiliary materials are available in the HTML. doi:10.1029/2006JG000236.
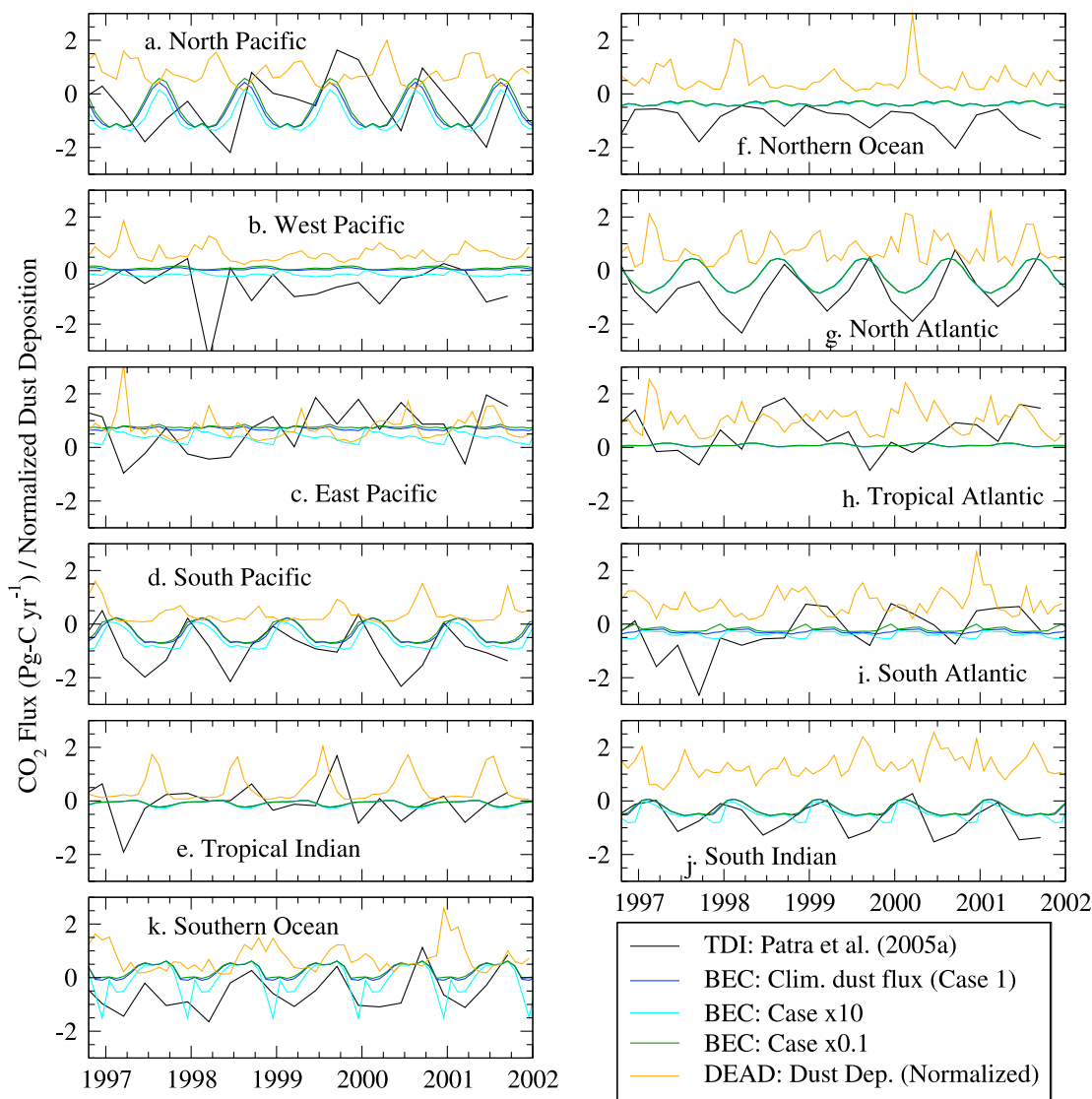
Figure 7. Regional time series in monthly estimated sea-air CO$_2$ fluxes from the TDI model for 11 ocean regions (see Figure 1b for region names) and the cyclostationary BEC simulations for the three different atmospheric dust input scenarios. BEC fluxes are sampled 1 year following the dust step-function perturbation (see auxiliary material Figure S1 for the fluxes after 5 years). The DEAD model interannual variability in dust deposition amounts, normalized by 2σ, are also shown.

the iron inputs and the BEC modeled seasonal cycle is smaller than that obtained by TDI model.

[23] For the North Pacific and South Atlantic regions, we find that the Case-x0.1 BEC simulation produced somewhat larger seasonal cycles compared to Case-x1 or Case-x10. However, the North Pacific seasonal cycles (amplitude and phase) are in fairly good agreement between the two models. An interesting finding is that for the South Atlantic region the seasonal flux amplitude and phase of TDI model fluxes are in near perfect match with that of BEC model simulations after 5 years if the atmospheric dust input is reduced by one tenth (Case-x0.1; see auxiliary material Figure S1).

[24] The interannual variability in dust deposition from the MATCH/NCEP/DEAD model is also shown in Figure 7 (see also Figure 2 and auxiliary material Figure S1). The

absolute magnitude of dust deposition to the Tropical Pacific and Southern Ocean is small but the relative interannual variability can be large (Figures 7c and 7k). There is some indication of negative CO$_2$ flux anomalies (uptake) from TDI following increased dust deposition. For some ocean basins, atmospheric deposition of nutrients and micronutrients could result from large-scale biomass burning [e.g., *Abram et al.*, 2003] or fossil fuel combustion [e.g., *Chuang et al.*, 2005], which are not accounted for here. In general, all the tropical land areas exhibit large interannual and decadal variabilities in biomass burning in relation with the prevalent climate conditions associated with the ENSO cycle [e.g., *Roedenbeck et al.*, 2003; *Patra et al.*, 2005b]. Plausible temporal correlations are found between monthly mean DEAD/MATCH/NCEP dust depositions and TDI modeled CO$_2$ fluxes for the North Pacific ($r^2 = -0.74$), Northern Ocean ($r^2 = -0.59$)

and Southern Ocean ($r^2 = -0.56$) with elevated CO_2 uptake lagging a few months behind periods with elevated dust deposition. Interestingly, the seasonal cycle trough in CO_2 fluxes always follows the peak in dust deposition cycle in these regions. However, the observed sea-air CO_2 fluxes convolves both dust and climate variability, and a more comprehensive analysis will be required to relate definitively dust and sea-air CO_2 flux variations.

4. Conclusions

[25] The atmospheric time-dependent inverse model (TDI) derived ocean CO_2 fluxes are compared with those from the ocean BEC model simulations under three different levels of iron input to the oceans from atmospheric aerosols. The mean annual global and regional flux amplitudes estimated using the TDI and BEC models are in overall good agreement with those estimated using shipboard measurements, within their respective uncertainties (Table 1). There is also broad agreement of the estimated TDI and BEC seasonal cycles for most of the extratropical regions. Case studies of the BEC model with different dust inputs exhibit changes in ocean CO_2 exchange in some HNLC regions that are similar in magnitude to the interannual variability estimated from the TDI model. The TDI model results also include variations due to interannual climate variability not accounted for in the BEC simulations where a physical surface forcing climatology is used. The results suggest that a greater input of iron to the Southern Ocean and Tropical Pacific, compared with that from the DEAD/ MATCH/NCEP dust deposition climatology, would result in more consistent CO_2 fluxes from the BEC and TDI models. On the other hand, less iron input to the South Atlantic and North Pacific would better match the BEC and TDI modeled net fluxes and seasonal cycle (Figure 7 and auxiliary material Figure S1).

[26] These findings point to regions where the dust deposition climatology may be under or overestimated, to deficiencies in the ocean model estimates of air-sea exchange, or areas where the TDI under or overestimates the air-sea flux. The tropical Pacific is an area with excessive ocean model flux of DIC and nutrients to surface waters [*Gnanadesikan et al.*, 2002; *Doney et al.*, 2004]. This factor may explain some of the discrepancies in this region. Assumptions about the solubility and bioavailability of iron within mineral dust also impact our ocean simulations, and are not well constrained. However, the construction of dust input maps are severely data limited, so any improvement is likely to take a broader effort than just the modeling community (e.g., see review by *Mahowald et al.* [2005]). The interannual variability in dust input is also linked to the regional patterns of rainfall (over the land for emission and over the oceans for deposition), which must be considered for future simulations for a more realistic representation of interannual variability in biogeochemical modeling of CO_2 fluxes. The other emerging view from this comparison is that the oceanic fluxes are derived fairly well by the TDI model used here, and inverse model results for the oceanic regions may not be as under constrained as thought previously. Thus the two approaches mutually support each other to some extent. The increase in atmospheric CO_2 observation network over the last two decades has played a major role in this improvement in TDI modeling [*Patra et al.*, 2005a, 2006]. Thus we believe a better network for measuring dust input to the oceans will allow us to make significant progress in our understanding of land-ocean linkages and regional to global-scale carbon cycling.

References

Abram, N. J., M. K. Gagan, M. T. McCulloch, J. Chappell, and W. S. Hantoro (2003), Coral reef death during the 1997 Indian Ocean dipole linked to Indonesian wildfires, *Science*, *301*, 952–955.

Angert, A., S. Biraud, C. Bonfils, C. C. Henning, W. Buermann, J. Pinzon, C. J. Tucker, and I. Fung (2005), Drier summers cancel out the CO_2 uptake enhancement induced by warmer springs, *Proc. Natl. Acad. Sci. U. S. A.*, *102*, 10,823–10,827.

Archer, D. E., and K. Johnson (2000), A model of the iron cycle in the ocean, *Global Biogeochem. Cycles*, *14*(1), 269–280.

Asner, G. P., D. E. Knapp, E. N. Broadbent, P. J. C. Oliveira, M. Keller, and J. N. Silva (2005), Selective logging in the Brazilian Amazon, *Science*, *310*, 480–482.

Bousquet, P., P. Peylin, P. Ciais, C. Le Quéré, P. Friedlingstein, and P. Tans (2000), Regional changes in carbon dioxide fluxes of land and ocean since 1980, *Science*, *290*, 1342–1346.

Boyd, P. W., and S. C. Doney (2002), Modelling regional responses by marine pelagic ecosystems to global climate change, *Geophys. Res. Lett.*, *29*(16), 1806, doi:10.1029/2001GL014130.

Chuang, P. Y., R. M. Duvall, M. M. Shafer, and J. J. Schauer (2005), The origin of water soluble particulate iron in the Asian atmospheric outflow, *Geophys. Res. Lett.*, *32*, L07813, doi:10.1029/2004GL021946.

Ciais, P., et al. (2005), Europe-wide reduction in primary productivity caused by the heat and drought in 2003, *Nature*, *437*, 529–533.

Collins, W. D., et al. (2006), The Community Climate System Model: CCSM3, *J. Clim.*, *19*(11), 2122–2143.

Cox, P. M., R. A. Betts, C. D. Jones, S. A. Spall, and I. J. Totterdell (2000), Acceleration of global warming due to carbon cycle feedbacks in a coupled climate model, *Nature*, *408*, 184–187.

Dilling, L., S. C. Doney, J. Edmonds, K. R. Gurney, R. Harriss, D. Schimel, B. Stephens, and G. Stokes (2003), The role of carbon cycle observations and knowledge in carbon management, *Annu. Rev. Environ. Resour.*, *28*, 521–558, doi:10.1146/annurev.energy.28.011503.163443.

Doney, S. C., et al. (2004), Evaluating global ocean carbon models: The importance of realistic physics, *Global Biogeochem. Cycles*, *18*, GB3017, doi:10.1029/2003GB002150.

Dore, J. E., R. Lukas, D. W. Sadler, and D. M. Karl (2003), Climate-driven changes to the atmospheric CO_2 sink in the subtropical North Pacific Ocean, *Nature*, *424*, 754–757.

Feely, R. A., R. Wanninkhof, T. Takahashi, and P. Tans (1999), Influence of El Niño on the equatorial Pacific contribution of atmospheric CO_2 accumulation, *Nature*, *398*, 597–601.

Friedlingstein, P., et al. (2006), Climate-carbon cycle feedback analysis: Results from the C^4MIP model intercomparison, *J. Clim.*, *19*(14), 3337–3353.

Fung, I. Y., S. K. Meyn, I. Tegen, S. C. Doney, J. G. John, and J. K. B. Bishop (2000), Iron supply and demand in the upper ocean, *Global Biogeochem. Cycles*, *14*, 281–295.

Fung, I., S. C. Doney, K. Lindsay, and J. John (2005), Evolution of carbon sinks in a changing climate, *Proc. Natl. Acad. Sci. U. S. A.*, *102*, 11,201–11,206, doi:10.1073/pnas.0504949102.

Ginoux, P., M. Chin, I. Tegen, J. M. Prospero, B. N. Holben, O. Dubovik, and S.-J. Lin (2001), Sources and distribution of dust aerosols with the GOCART model, *J. Geophys. Res.*, *106*, 20,255–20,273.

GLOBALVIEW-CO_2 (2004), *Cooperative Atmospheric Data Integration Project–Carbon Dioxide*, [CD-ROM], Natl. Oceanic Atmos. Administration, Clim. Monit. and Diagnostics Lab., Boulder, Colo. [Available on Internet via anonymous FTP to ftp.cmdl.noaa.gov, Path: ccg/co2/ GLOBALVIEW].

Gnanadesikan, A., R. D. Slater, N. Gruber, and J. L. Sarmiento (2002), Oceanic vertical exchange and new production: A comparison between models and observations, *Deep Sea Res., Part II*, *49*, 363–401.

Gregg, W. W., N. W. Casey, and C. R. McClain (2005), Recent trends in global ocean chlorophyll, *Geophys. Res. Lett.*, *32*, L03606, doi:10.1029/2004GL021808.

Gruber, N., C. D. Keeling, and N. R. Bates (2002), Interannual variability in the North Atlantic Ocean carbon sink, *Science*, *298*, 2374–2378.

Gurney, K. R., et al. (2004), Transcom 3 inversion intercomparison: Model mean results for the estimation of seasonal carbon sources and sinks, *Global Biogeochem. Cycles*, *18*, GB1010, doi:10.1029/2003GB002111.

Hand, J. L., N. Mahowald, Y. Chen, R. Siefert, C. Luo, A. Subramaniam, and I. Fung (2004), Estimates of soluble iron from observations and a global mineral aerosol model: Biogeochemical implications, *J. Geophys. Res.*, *109*, D17205, doi:10.1029/2004JD004574.

Jickells, T. D., et al. (2005), Global iron connections between desert dust, ocean biogeochemistry and climate, *Science*, *308*, 67–71.

Johnson, K. S., R. M. Gordon, and K. H. Coale (1997), What controls dissolved iron concentrations in the world ocean?, *Mar. Chem.*, *57*, 137–161.

Keeling, C. D., T. P. Whorf, M. Wahlen, and J. van der Plicht (1995), Interannual extremes in the rate of rise of atmospheric carbon dioxide since 1980, *Nature*, *375*, 666–670.

Kistler, R., et al. (2001), The NCEP-NCAR 50-year reanalysis: Monthly means CD-ROM and documentation, *Bull. Am. Meteorol. Soc.*, *82*, 247–267.

Koch, D., T. C. Bond, D. Streets, N. Unger, and G. R. van der Werf (2007), Global impacts of aerosols from particular source regions and sectors, *J. Geophys. Res.*, *112*, D02205, doi:10.1029/2005JD007024.

Lam, P. J., J. K. Bishop, C. C. Henning, A. Marcus, G. A. Waychunas, and I. Y. Fung (2006), Wintertime phytoplankton bloom in the subarctic Pacific supported by continental margin iron, *Global Biogeochem. Cycles*, *20*, GB1006, doi:10.1029/2005GB002557.

Lee, K., R. Wanninkhof, T. Takahashi, S. C. Doney, and R. A. Feely (1998), Low interannual variability in recent oceanic uptake of atmospheric carbon dioxide, *Nature*, *396*, 155–159.

Le Quéré, C., J. C. Orr, P. Monfray, O. Aumont, and G. Madec (2000), Interannual variability of the oceanic sink of CO₂ from 1979 through 1997, *Global Biogeochem. Cycles*, *14*, 1247–1266.

Le Quéré, C., et al. (2003), Two decades of ocean CO₂ sink and variability, *Tellus, Ser. B.*, *55*, 649–656.

Lucht, W., I. C. Prentice, R. B. Myneni, S. Sitch, P. Friedlingstein, W. Cramer, P. Bousquet, W. Buermann, and B. Smith (2002), Climatic control of the high-latitude vegetation greening trend and Pinatubo effect, *Science*, *296*, 1687–1689.

Luo, C., N. M. Mahowald, and J. del Corral (2003), Sensitivity study of meteorological parameters on mineral aerosol mobilization, transport, and distribution, *J. Geophys. Res.*, *108*(D15), 4447, doi:10.1029/2003JD003483.

Mahowald, N. M., P. Rasch, B. Eaton, S. Whittlestone, and R. Prinn (1997), Transport of ²²²radon to the remote troposphere using MATCH and assimilated winds from ECMWF and NCEP/NCAR, *J. Geophys. Res.*, *102*, 28,139–28,152.

Mahowald, N. M., C. S. Zender, C. Luo, D. Savoie, O. Torres, and J. del Corral (2002), Understanding the 30-year Barbados desert dust record, *J. Geophys. Res.*, *107*(D21), 4561, doi:10.1029/2002JD002097.

Mahowald, N. M., C. Luo, J. del Corral, and C. Zender (2003), Interannual variability in atmospheric mineral aerosols from a 22-year model simulation and observational data, *J. Geophys. Res.*, *108*(D12), 4352, doi:10.1029/2002JD002821.

Mahowald, N., A. Baker, G. Bergametti, N. Brooks, R. Duce, T. Jickells, N. Kubilay, J. Prospero, and I. Tegen (2005), The atmospheric global dust cycle and iron inputs to the ocean, *Global Biogeochem. Cycles*, *19*, GB4025, doi:10.1029/2004GB002402.

Martin, J. H., R. M. Gordon, and S. E. Fitzwater (1991), The case for iron, *Limnol. Oceanogr.*, *36*, 1793–1802.

McKinley, G. A., M. J. Follows, and J. C. Marshall (2004), Mechanisms of air-sea CO₂ flux variability in the equatorial Pacific and the North Atlantic, *Global Biogeochem. Cycles*, *18*, GB2011, doi:10.1029/2003GB002179.

McKinley, G. A., et al. (2006), North Pacific carbon cycle response to climate variability on seasonal to decadal timescales, *J. Geophys. Res.*, *111*, C07S06, doi:10.1029/2005JC003173.

Moore, J. K., S. C. Doney, D. M. Glover, and I. Y. Fung (2002), Iron cycling and nutrient-limitation patterns in surface waters of the world ocean, *Deep Sea Res., Part II*, *49*, 463–507.

Moore, J. K., S. C. Doney, and K. Lindsay (2004), Upper ocean ecosystem dynamics and iron cycling in a global three-dimensional model, *Global Biogeochem. Cycles*, *18*, GB4028, doi:10.1029/2004GB002220.

Moore, J. K., S. C. Doney, K. Lindsay, N. Mahowald, and A. F. Michaels (2006), Nitrogen fixation amplifies the ocean biogeochemical response to decadal timescale variations in mineral dust deposition, *Tellus, Ser. B*, *58*, 560–572.

Nemani, R. R., C. D. Keeling, H. Hashimoto, W. M. Jolly, S. C. Piper, C. J. Tucker, R. B. Myneni, and S. W. Running (2003), Climate-driven increases in global terrestrial net primary production from 1982 to 1999, *Science*, *300*, 1560–1563.

Obata, A., and Y. Kitamura (2003), Interannual variability of the sea-air exchange of CO₂ from 1961 to 1998 simulated with a global ocean circulation-biogeochemistry model, *J. Geophys. Res.*, *108*(C11), 3337, doi:10.1029/2001JC001088.

Patra, P. K., S. Maksyutov, M. Ishizawa, T. Nakazawa, T. Takahashi, and J. Ukita (2005a), Interannual and decadal changes in the sea-air CO₂ flux from atmospheric CO₂ inverse modeling, *Global Biogeochem. Cycles*, *19*, GB4013, doi:10.1029/2004GB002257.

Patra, P. K., M. Ishizawa, S. Maksyutov, T. Nakazawa, and G. Inoue (2005b), Role of biomass burning and climate anomalies for land-atmosphere carbon fluxes based on inverse modeling of atmospheric CO₂, *Global Biogeochem. Cycles*, *19*, GB3005, doi:10.1029/2004GB002258.

Patra, P. K., S. E. Mikaloff-Fletcher, K. Ishijima, S. Maksyutov, and T. Nakazawa (2006), Comparison of CO₂ fluxes estimated using atmospheric and oceanic inversions, and role fluxes in simulating atmospheric CO₂ concentrations, *Atmos. Chem. Phys. Disc.*, *6*, 6801–6823.

Peylin, P., P. Bousquet, C. Le Quéré, S. Sitch, P. Friedlingstein, G. McKinley, N. Gruber, P. Rayner, and P. Ciais (2005), Multiple constraints on regional CO₂ flux variations over land and oceans, *Global Biogeochem. Cycles*, *19*, GB1011, doi:10.1029/2003GB002214.

Prentice, I. C., et al. (2001), The carbon cycle and atmospheric carbon dioxide (Chap. 3), in *Climate Change 2001: The Scientific Basis*, edited by J. T. Houghton et al., pp. 183–237, Cambridge Univ. Press, New York.

Rasch, P., N. Mahowald, and B. Eaton (1997), Representations of transport, convection and the hydrologic cycle in chemical transport models: Implications for the modeling of short-lived and soluble species, *J. Geophys. Res.*, *102*, 28,127–28,138.

Rayner, P. J., I. G. Enting, R. J. Francey, and R. Langenfelds (1999), Reconstructing the recent carbon cycle from atmospheric CO₂, δ^{13}C and O₂/N₂ observations, *Tellus, Ser. B.*, *51*, 213–232.

Rengarajan, R., and M. M. Sarin (2004), Atmospheric deposition fluxes of ⁷Be, ²¹⁰Pb and chemical species to the Arabian Sea and Bay of Bengal, *Indian J. Mar. Sci.*, *33*(1), 56–64.

Roedenbeck, C., S. Houweling, M. Gloor, and M. Heimann (2003), CO₂ flux history 1982–2001 inferred from atmospheric data using a global inversion of atmospheric transport, *Atmos. Chem. Phys.*, *3*, 1919–1964.

Sabine, C. L., R. Wanninkhof, R. M. Key, C. Goyet, and F. J. Millero (2000), Seasonal CO₂ fluxes in the tropical and subtropical Indian Ocean, *Mar. Chem.*, *72*, 33–53.

Sarmiento, J. L., N. Gruber, M. A. Brzezinski, and J. P. Dunne (2004), High-latitude controls of thermocline nutrients and low latitude biological productivity, *Nature*, *427*, 56–60.

Satheesh, S. K., and V. Ramanathan (2000), Large differences in tropical aerosol forcing at the top of the atmosphere and Earth's surface, *Nature*, *405*, 60–63.

Syvitski, J. P. M., C. J. Voeroesmarty, A. J. Kettner, and P. Green (2005), Impact of humans on the flux of terrestrial sediment to the global coastal ocean, *Science*, *308*, 376–380.

Takahashi, T., et al. (2002), Global sea-air CO₂ flux based on climatological surface ocean pCO₂, and seasonal biological and temperature effects, *Deep Sea Res., Part II*, *49*, 1601–1622.

Takahashi, T., S. C. Sutherland, R. A. Feely, and C. Cosca (2003), Decadal variation of the surface water pCO₂ in the western and central equatorial Pacific, *Science*, *302*, 852–856.

Tegen, I., and R. Miller (1998), A general circulation model study on the interannual variability of soil dust aerosol, *J. Geophys. Res.*, *103*, 25,975–25,995.

Tegen, I., P. Hollrig, M. Chin, I. Fung, D. Jacob, and J. Penner (1997), Contribution of different aerosol species to the global aerosol extinction optical thickness: Estimates from model results, *J. Geophys. Res.*, *102*, 23,895–23,915.

Uematsu, M., A. Yoshikawa, H. Muraki, K. Arao, and I. Uno (2002), Transport of mineral and anthropogenic aerosols during a Kosa event over East Asia, *J. Geophys. Res.*, *107*(D7), 4059, doi:10.1029/2001JD000333.

van der Werf, G. R., J. T. Randerson, L. Giglio, G. J. Collatz, P. S. Kasibhatla, and A. F. Arellano Jr. (2006), Interannual variability in global biomass burning emissions from 1997 to 2004, *Atmos. Chem. Phys.*, *6*, 3423–3441.

Wanninkhof, R. (1992), Relationship between wind speed and gas exchange, *J. Geophys. Res.*, *97*, 7373–7382.

Wetzel, P., A. Winguth, and E. Maier-Reimer (2005), Sea-to-air CO₂ flux from 1948 to 2003: A model study, *Global Biogeochem. Cycles*, *19*, GB2005, doi:10.1029/2004GB002339.

Zender, C. S., H. Bian, and D. Newman (2003), Mineral Dust Entrainment and Deposition (DEAD) model: Description and 1990s dust climatology, *J. Geophys. Res.*, *108*(D14), 4416, doi:10.1029/2002JD002775.

————————————

S. C. Doney, Department of Marine Chemistry and Geochemistry, Woods Hole Oceanographic Institution, Woods Hole, MA 02543-1543, USA. (sdoney@whoi.edu)

N. Mahowald, National Center for Atmospheric Research, P.O. Box 3000, Boulder, CO 80307-3000, USA. (mahowald@ucar.edu)

J. K. Moore, Earth System Science, University of California, Irvine, 3214 Croul Hall, Irvine, CA 92697-3100, USA. (jkmoore@uci.edu)

T. Nakazawa, Center for Atmospheric and Oceanic Studies, Tohoku University, Sendai 980-8578, Japan. (nakazawa@mail.tains.tohoku.ac.jp)

P. K. Patra, Frontier Research Center for Global Change, Japan Agency for Marine-Earth Science and Technology, 3173-25 Showa-machi, Yokohama 236-0001, Japan. (prabir@jamstec.go.jp)

M. Uematsu, Center for International Cooperation, Ocean Research Institute, University of Tokyo, 1-15-1 Minamidai, Nakano, Tokyo 164-8639, Japan. (uematsu@ori.u-tokyo.ac.jp)